Available online at www.sciencedirect.com
ScienceDirect
Acta Materialia 58 (2010) 4723–4729
Acta MATERIALIA
www.elsevier.com/locate/actamat

Evolution of the relaxation spectrum during the strain glass transition of $Ti_{48.5}Ni_{51.5}$ alloy

Yu Wang [a,b,c], Yumei Zhou [a,b,d], Jian Zhang [b,d], Xiangdong Ding [b,d], Sen Yang [b,c], Xiaoping Song [b,c], Xiaobing Ren [a,b,*], Kazuhiro Otsuka [a]

[a] National Institute for Materials Science, 1-2-1 Sengen, Tsukuba, Ibaraki 305-0047, Japan
[b] Multi-Disciplinary Materials Research Center, Frontier Institute of Science and Technology, Xi'an Jiaotong University, Xi'an 710049, People's Republic of China
[c] Department of Physics, Xi'an Jiaotong University, Xi'an 710049, People's Republic of China
[d] State Key Laboratory for Mechanical Behavior of Materials, Xi'an Jiaotong University, Xi'an 710049, People's Republic of China

Received 22 January 2010; received in revised form 1 April 2010; accepted 4 May 2010
Available online 10 June 2010

Abstract

The glass transition is essentially a kinetics governed freezing transition and is characterized by a broad distribution of relaxation times. Quantitative determination of the relaxation spectrum of a glass system is thus crucial in understanding the glassy behavior. In this study the temperature evolution of the relaxation spectrum of a new glass system, a $Ti_{48.5}Ni_{51.5}$ strain glass, was obtained, which provides a full description of the kinetic relaxation behavior in this system. Our results show that the typical glassy features of strain glass can be readily understood from the relaxation spectrum. We further found that the system shows a transition from Vogel–Fulcher kinetics to Arrhenius kinetics around the freezing temperature. Moreover, our result answers some important questions, such as why the onset of non-ergodicty starts above the freezing temperature and why the precursor state with a static tweed microstructure appears to be ergodic prior to the normal martensitic transformation.

Keywords: Martensitic phase transformation; Shape memory alloys; Dynamic mechanical analysis; Point defects; Strain glass

1. Introduction

Glass is a frozen or "quenched-in" disordered state with local order only, which is usually found in "frustrated" systems with random defects or impurities [1,2]. It is characterized by a freezing transition where the final low temperature state is a frozen non-equilibrium state. Since the glass system fails to achieve equilibrium, the glass transition cannot be considered a thermodynamic phase transition and thus the physics of this system are beyond the framework of classical statistical physics.

Numerous studies [3–5] have demonstrated that the glass transition is actually a kinetics governed freezing transition. A slowing down of the kinetic process (i.e. relaxation behavior) results in the glass transition. The kinetic relaxation of a glass can be fully described by a relaxation spectrum, which is a probability distribution of different Debye-like relaxation processes with different relaxation times [4]. Such a spectrum makes it possible to explore the relative "weight" of each relaxation time in the whole relaxation spectrum. Analysis of the spectrum can yield important information about the glass, which can be used to understand all the glass signatures, such as the frequency dependence of the properties and non-ergodicity. For such reasons quantitative determination of the relaxation spectrum of various glasses has attracted substantial interest over recent years [6–10].

* Corresponding author at: Address: National Institute for Materials Science, 1-2-1 Sengen, Tsukuba, Ibaraki 305-0047, Japan. Tel.: +81 29 859 2731; fax: +81 29 859 2701.
E-mail address: ren.xiaobing@nims.go.jp (X. Ren).

1359-6454/$36.00 © 2010 Acta Materialia Inc. Published by Elsevier Ltd. All rights reserved.
doi:10.1016/j.actamat.2010.05.009

Very recently a new glass phenomenon called strain glass [11–15] has been found in the "non-transforming" composition regime of the well-known $Ti_{50-x}Ni_{50+x}$ martensitic system (for $x \geqslant 1.5\%$). Strain glass is a new state of matter and is characterized by frozen locally ordered lattice strains, i.e. random nanosized strain domains. Strain glass was created by doping sufficient point defects (excess Ni) into a pure martensitic system. These point defects are distributed randomly in the lattice and produce random local stresses, which result in nanoscale strain ordered domains and produce high energy barriers to flipping of these nanodomains [11–13]. Although these nanodomains have a tendency to transform into a long-range strain ordered state (martensite) on cooling, forming martensite by forcing numerous defect-dictated nanodomains to flip into the same orientation will encounter large energy barriers caused by point defects. As a result, the system cannot transform into martensite but instead transforms into a strain glass with randomly distributed nanosized strain domains. The strain glass alloy cannot undergo a spontaneous martensitic transition, however, a recent study [12] has shown that it can exhibit a shape memory effect and superelasticity, which is unexpected based on the classical theory of martensitic transition. In situ X-ray diffraction observations also proved that the origin of the shape memory effect and superelasticity of a strain glass stems from the stress-induced strain glass to martensite transition, which is quite different from that of a normal martensitic alloy. The finding of these novel properties of strain glass makes it a subject of both fundamental interest and practical importance.

Previous experimental evidence about the frequency-dependent dynamic mechanical anomaly [11] and the breaking down of ergodicity [13] qualitatively confirmed that the strain glass transition is governed by kinetics. However, a full quantitative description of the kinetic slowing down process during the strain glass transition is still lacking. In this study we determined the relaxation spectrum of a strain glass $Ti_{48.5}Ni_{51.5}$ by fitting experimentally measured complex compliance data to a phenomenological model, which will provide crucial information about the kinetic relaxation of the system over the full time scale, from very short time of 10^{-15} s to very long time of 10^{15} s. In addition, we also obtained the temperature evolution of the relaxation spectrum, which reveals how kinetic relaxation of the system evolves during the strain glass transition.

As will be shown later, evolution of the relaxation spectrum of a strain glass explains two key features of strain glasses: (i) frequency-dependent dynamic freezing and (ii) a breakdown of ergodicity. In addition, the relaxation spectrum of the strain glass reveals a new glassy feature: a transition from Vogel–Fulcher relaxation behavior to Arrhenius relaxation behavior around the freezing temperature T_g. Finally, quantitative kinetics information about the strain glass also provides the answers to two important questions: (1) why the onset of non-ergodicty starts above the freezing temperature T_g, as shown in a previous study [13], and (2) why the "ergodic" precursory state prior to the martensitic transition [15] shows a "static" tweed pattern [16], or nanoclusters [17,18], as observed by transmission electron microscopy (TEM).

2. Model of mechanical relaxation in strain glass

The relaxation spectrum of many glasses, such as the magnetic relaxation spectrum of cluster–spin glasses and the dielectric relaxation spectrum of relaxor ferroelectrics, can be expressed as a superimposition of numerous individual Debye relaxation processes with certain distribution probabilities. The mechanical relaxation spectrum of strain glasses should follow the same definition, since strain glasses show striking similarities to cluster–spin glasses and relaxor ferroelectrics [12,13]. Thus the mechanical relaxation spectrum of strain glasses can be defined as a probability distribution function $g(\ln\tau)$ of relaxation time τ which satisfies the same analytical equation given by Binder and Young [4]:

$$\frac{J^*(\omega)-J_\infty}{J_S-J_\infty}=\int_{\tau=0}^{\tau\to\infty}\frac{1}{1+i\omega\tau}g(\ln\tau)d(\ln\tau), \tag{1}$$

where J_S and J_∞ are the static compliance and the compliance at infinite frequency, respectively. $J^*(\omega)$ is the frequency (ω)-dependent complex compliance. It can be expressed as:

$$J^*(\omega)=J'(\omega)+iJ''(\omega), \tag{2}$$

in which $J'(\omega)$ and $J''(\omega)$ are the storage and loss compliances and can be measured experimentally. The analytical expression of the relaxation spectrum $g(\ln\tau)$ in Eq. (1) can be obtained through phenomenological models [19,20] of the relaxation behavior. Representative ones are the Cole–Davidson, Cole–Cole and Havriliak–Negami equations [21,22], which are empirical modifications of the Debye equation. In this study we chose the Havriliak–Negami model to obtain the relaxation spectrum of a strain glass, because in principle it can describe any relaxation process [22]. The Havriliak–Negami equation is analytically expressed as:

$$\frac{J^*(\omega)-J_\infty}{J_S-J_\infty}=\frac{1}{[1+(i\omega\tau_0)^\alpha]^\gamma}, \tag{3}$$

where α, γ are exponential factors and τ_0 is the characteristic relaxation time. By combining Eqs. (1) and (3) the analytical expression of the distribution function $g(\ln\tau)$ for a strain glass can be expressed as:

$$g(\ln\tau)=\frac{1}{\pi}\frac{(\tau/\tau_0)^{\alpha\gamma}\sin(\gamma\theta)}{[(\tau/\tau_0)^{2\alpha}+2(\tau/\tau_0)^\alpha\cos(\alpha\pi)+1]^{\gamma/2}}, \tag{4}$$

where θ is expressed by:

$$\theta=\arctan\left|\frac{\sin(\alpha\pi)}{(\tau/\tau_0)^\alpha+\cos(\alpha\pi)}\right|. \tag{5}$$

Eqs. (4) and (5) show that the distribution function $g(\ln\tau)$ can be determined if the factors α, γ and τ_0 are known.

The factors α, γ and τ_0 can be obtained by fitting the experimentally measured storage compliance $J'(\omega)$ vs. loss compliance $J''(\omega)$ curve, called a Cole–Cole plot, to Eq. (3). For convenience of fitting, Eq. (3) is usually expressed equivalently as:

$$J'(\omega)=J_\infty+(J_S-J_\infty)\frac{\cos(\gamma\varphi)}{\{1+2(\omega\tau_0)^\alpha\sin[\frac{\pi}{2}(1-\alpha)]+(\omega\tau_0)^{2\alpha}\}^{\gamma/2}}, \quad (6)$$

$$J''(\omega)=(J_S-J_\infty)\frac{\sin(\gamma\varphi)}{\{1+2(\omega\tau_0)^\alpha\sin[\frac{\pi}{2}(1-\alpha)]+(\omega\tau_0)^{2\alpha}\}^{\gamma/2}}, \quad (7)$$

with

$$\varphi=\arctan\left\{\frac{(\omega\tau_0)^\alpha\cos[\frac{\pi}{2}(1-\alpha)]}{1+(\omega\tau_0)^\alpha\sin[\frac{\pi}{2}(1-\alpha)]}\right\}. \quad (8)$$

Through fitting the Cole–Cole plot ($J'(\omega)$ vs. $J''(\omega)$ curve) to both Eqs. (6) and (7) the factors α, γ and τ_0 for a strain glass can be obtained. Then the relaxation spectrum $g(\ln\tau)$ of the strain glass can also be determined.

3. Experimental procedure

The strain glass sample used in the present study was a commercial Ni-rich Ti–Ni alloy with a nominal composition $Ti_{48.5}Ni_{51.5}$. After removing the affected surface layer the sample, $55\times1.8\times1.2\ mm^3$, was annealed at 1237 K for 1 h in a evacuated quartz tube and subsequently quenched in room temperature water at a quenching rate of 500 K s^{-1}, which can prevent precipitation and produce a homogeneous supersaturated Ni-rich Ti–Ni solid solution.

As mentioned above, the relaxation spectrum of a strain glass can be obtained by fitting the Cole–Cole plot, i.e. $J'(\omega)$ vs. $J''(\omega)$ curve. Thus, the frequency-dependent storage compliance $J'(\omega)$ and loss compliance $J''(\omega)$ were measured over a frequency range of 0.05–40 Hz. The data ($J'(\omega)$, $J''(\omega)$) at frequency ω corresponds to one point of the Cole–Cole plot. In other words, each point ($J'(\omega)$, $J''(\omega)$) in the same Cole–Cole plot was measured at different frequencies. The dynamic measurement of the complex compliance of the strain glass was performed in a Q800 dynamic mechanical analyzer (DMA) from TA Instruments. A dual cantilever sample clamp was used. In order to clarify the change in the relaxation spectrum of the strain glass with temperature, the frequency dependencies of the storage and loss compliances were measured at several temperatures, which span from far above the freezing temperature T_g to well below T_g. In addition, the testing temperature range (138–198 K) was well below the temperature of point defect migration. All the above DMA measurements were performed using the same sample.

4. Results and discussion

The frequency dependence of the storage compliance $J'(\omega)$ and loss compliance $J''(\omega)$ for the $Ti_{48.5}5Ni_{51.5}$ strain glass are shown in Fig. 1a and b, which were measured in the temperature range 138–198 K. Each pair of curves ω vs. $J'(\omega)$ and ω vs. $J''(\omega)$ at the same temperature can be redrawn as the corresponding Cole–Cole plot in the $J'(\omega)$–$J''(\omega)$ plane, which is shown in Fig. 1c. The experimental data are shown as open square dots. Fig. 1c shows that the shape of the Cole–Cole plot of the strain glass changes with changing temperature. The Cole–Cole plot measured at 183 K is an arc shape. It can be well fitted to Eqs. (6) and (7), as indicated by the arc fitting curve in Fig. 1c. This demonstrates that Eqs. (6) and (7) are a suitable model for fitting the Cole–Cole plot of a strain glass. The Cole–Cole plots measured at other temperatures do not show a complete arc shape. This is because the dynamic mechanical measurements cannot scan a wide enough frequency range due to mechanical limitations. However, complete arc curves can be reasonably predicted by the fitting curves, as depicted in Fig. 1c.

The factors τ_0, α and γ at different testing temperatures were obtained by fitting corresponding Cole–Cole plots, shown in Fig. 2 and the inset. The temperature dependence of the characteristic relaxation time τ_0 is plotted in terms of a $1/T$ vs. $\ln\tau_0$ curve in Fig. 2. This shows that the kinetic relaxation behavior of the strain glass exhibits a dramatic change upon cooling. The $1/T$ vs. $\ln\tau_0$ curve of the strain glass conforms to the Vogel–Fulcher relationship $\tau=\tau_0\exp\{E_a/[k_B(T-T_0)]\}$ at high temperatures, as indicated by the concave curve. However, at lower temperatures it obeys the Arrhenius relationship, as shown by the straight line. The concave curve and straight line intersect at 161.6 K. This intersection temperature corresponds to the freezing temperature T_g of the $Ti_{48.5}Ni_{51.5}$ strain glass. It coincides with the value of T_g determined previously [13]. The corresponding characteristic relaxation time $\tau_0(T_g)$ at the freezing temperature is 4018 s. The term E_a/k_B (activation energy/Boltzmann constant) obtained by fitting to the Vogel–Fulcher relationship above T_g was about 157 K, which is very close to the value of T_g. The fact that the $1/T$ vs. $\ln\tau_0$ curve conforms to the Vogel–Fulcher relationship above T_g shows that kinetic relaxation of the strain glass has obvious freezing features. The dramatic transition from Vogel–Fulcher relaxation above T_g to Arrhenius relaxation below T_g is a glassy feature. This demonstrates that the two fundamentally different states – unfrozen and frozen – have quite different kinetic features. Interestingly, the similar change in relaxation behavior to that shown in Fig. 2 has been found in structural glasses [23] and dipole glasses [8]. Therefore, such a glassy feature during the kinetic freezing transition in glass systems would seem to be universal.

The relaxation spectrum of a $Ti_{48.5}Ni_{51.5}$ strain glass was obtained by substituting the α, γ and τ_0 values in Fig. 2 into Eq. (4). As presented in Fig. 3a, it is the probability distribution function $g(\ln\tau)$ over a wide relaxation time range from 10^{-15} to 10^{15} s. This allows the kinetics of a strain glass to be fully described from very short to very long time scales. Fig. 2 shows that the strain glass becomes frozen when the characteristic relaxation time is greater than

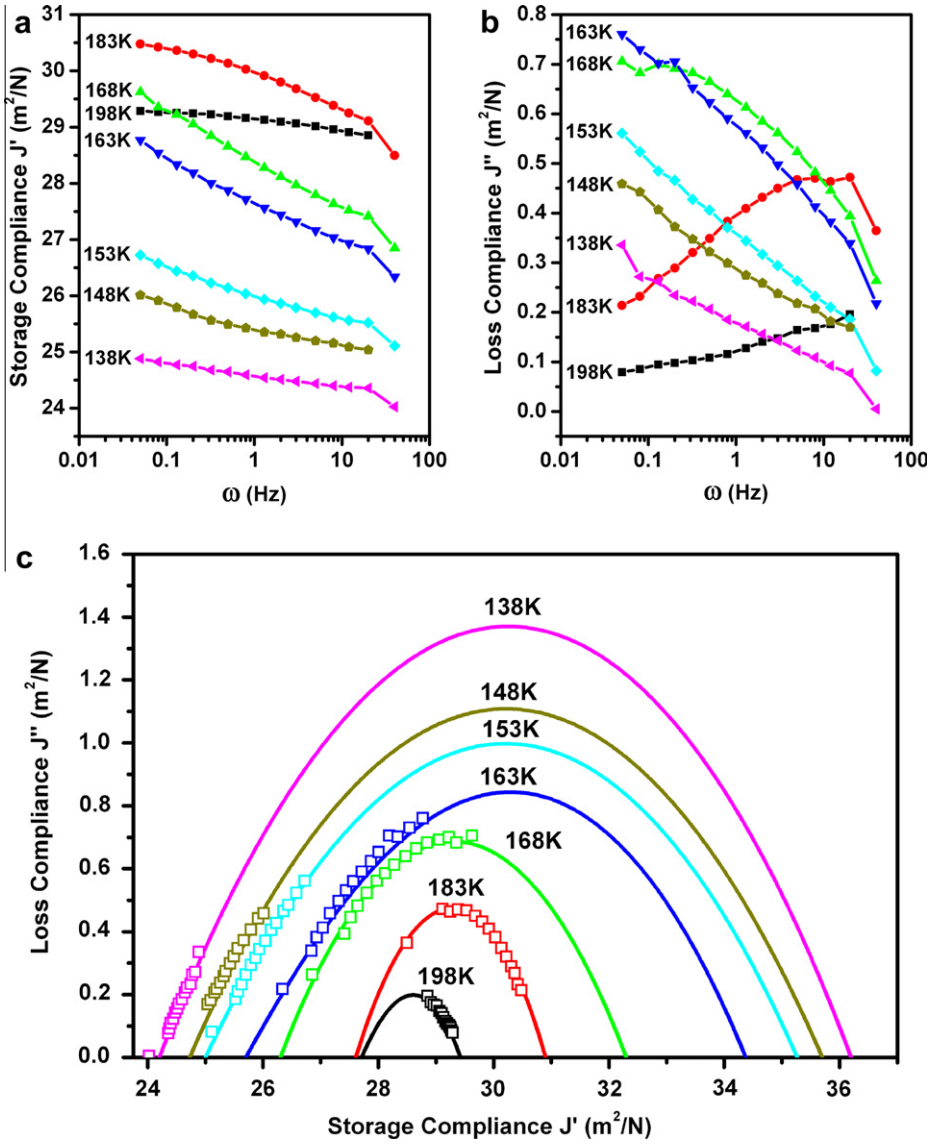

Fig. 1. The frequency dependence of (a) storage compliance $J'(\omega)$ and (b) loss compliance $J''(\omega)$ for $Ti_{48.5}Ni_{51.5}$ strain glass in the temperature range 138–198 K. (c) The experimental data (open square dots) of the Cole–Cole plots ($J'(\omega)$ vs. $J''(\omega)$) for $Ti_{48.5}Ni_{51.5}$ strain glass, which are redrawn from the ω vs. $J'(\omega)$ curves in (a) and ω vs. $J''(\omega)$ curves in (b) for the same temperatures. The solid curves are the corresponding fitting curves of Cole–Cole plots.

$\tau_0(T_g)$ (~4018 s). Thus, the relaxation spectrum of a strain glass can be divided by $\tau_0(T_g)$ into two regimes. One regime with a short relaxation time $\tau < \tau_0(T_g)$ forms the dynamic component of the relaxation spectrum, with fast kinetics. The regime with a long relaxation time $\tau > \tau_0(T_g)$ forms the quasi-static component, with slow kinetics.

The origin of the relaxation spectrum for the strain glass is as follows. Microscopically, the kinetic relaxation behavior of the strain glass represents the flipping of martensitic nanodomains. The flipping of a nanodomain requires the system to overcome a certain energy barrier E_a, and such a relaxation process is characterized by a corresponding characteristic relaxation time τ. Nano-domains of the same size have a fixed energy barrier E_a and characteristic relaxation time τ. In strain glasses there is a distribution of nanodomain sizes, for example the nanodomain size can vary from 1 to 40 nm in a Ti–Ni strain glass, as revealed by previous TEM observations [11]. Therefore, there exists a distribution of corresponding characteristic relaxation times in a strain glass, i.e. the relaxation spectrum. The probability of a fixed relaxation time τ in the relaxation spectrum is equivalent to the proportion of nanodomains with relaxation time τ in all the nanodomains. In the following we will show that the relaxation spectrum of a strain glass reflects its key glass features.

The shift of the peak position of the relaxation spectrum with temperature shown in Fig. 3a explains the frequency dispersion of the strain glass, i.e. a decrease in its storage modulus dip temperature $T_g(\omega)$ with decreasing testing frequency ω, as generally observed at the strain glass transition [11,12]. With decreasing temperature the relaxation spectrum of the system becomes more dominated by long

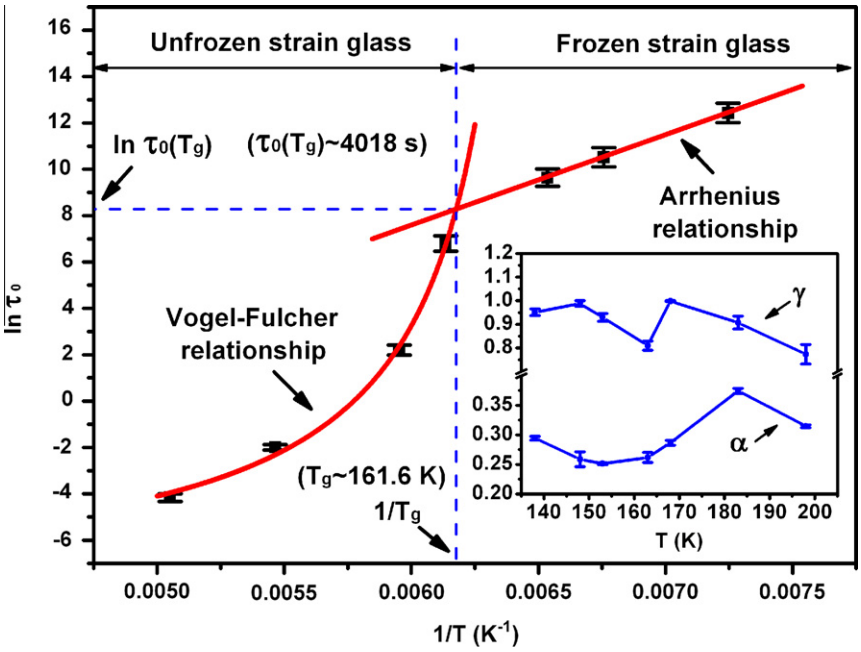

Fig. 2. The temperature dependence of the characteristic relaxation time τ_0 of $Ti_{48.5}Ni_{51.5}$ strain glass, which was obtained by fitting the data in Fig. 1. It shows that the relaxation behavior of the strain glass obeys the Vogel–Fulcher relationship above T_g but follows the Arrhenius relationship below T_g. The inset shows the temperature dependencies of the factors α and γ obtained by fitting.

relaxation times (as can be seen from the shift in the peak position towards longer times); as a result the system is more responsive to low frequency external excitations. This means that the low frequency modulus dip will occur at a lower temperature, as experimentally observed.

The change in the quasi-static component (long relaxation time regime) of the relaxation spectrum clearly reveals kinetic slowing down and an associated breakdown of ergodicity in the strain glass. The quasi-static component of the relaxation spectrum is defined by the shaded area depicted in the inset of Fig. 3b. As mentioned above, it is equivalent to the proportion of the nanodomains with $\tau > \tau_0(T_g)$ among all the nanodomains. In other words, the quasi-static component represents the proportion of the frozen martensitic nanodomains among all the nanodomains. As shown in Fig. 3b, the proportion of the quasi-static component is close to 0 at $T \gg T_g$. This demonstrates that flipping of the martensitic nanodomains is very fast and almost no quasi-static nanodomains are present. Thus the system is ergodic (unfrozen) in this temperature range. With decreasing temperature the proportion of quasi-static component increases continuously and shows a rapid increase around the freezing temperature T_g. Since the proportion of the quasi-static component has become large enough at T_g, flipping of most of the nanodomains starts to slow down and the global ergodicity of the system starts to break down. On further cooling to $T \ll T_g$, the proportion of the quasi-static component approaches 1. This suggests that most of the martensitic nanodomains become static and frozen and the ergodicity of the system is completely broken. From the above it can be seen that the non-ergodicity of strain glasses and the strain glass transition stem from the increase in the "weight" of the long relaxation time component. This characteristic is quite different from that of most thermodynamic transitions, which do not stem from a slowing down of the kinetics but from macroscopic symmetry breaking of the corresponding order parameter.

It should be emphasized that, within tens of Kelvin above T_g, although the relaxation spectrum is essentially dominated by short relaxation times and the system appears ergodic as a whole, the quasi-static component is still significant, as shown in Fig. 3b. This means that a considerable number of martensitic nanodomains, a maximum proportion of 30%, could remain static over a time scale as long as 4018 s ($\tau_0(T_g)$), as depicted schematically in the inset of Fig. 3b. This results in a partial breakdown of ergodicity and the freezing of a small number of martensitic nanodomains above T_g. This explains why the onset of non-ergodicty started above T_g in zero field cooling/field cooling (ZFC/FC) measurements [13] and why static nanodomains appeared in the unfrozen strain glass state at $T > T_g$ [11].

Quantitative calculation of the quasi-static component for the unfrozen strain glass ($T > T_g$) can also explain an important "paradox" about the nature of the precursor state, with a pre-martensitic tweed pattern or nanodomains [16–18]. TEM images show that the tweed or nanodomains are static above the martensitic transition temperature M_s, which suggests that the precursor state is static in nature. Previous theoretical studies [24–26] also suggested that the tweedy precursor state is non-ergodic. However,

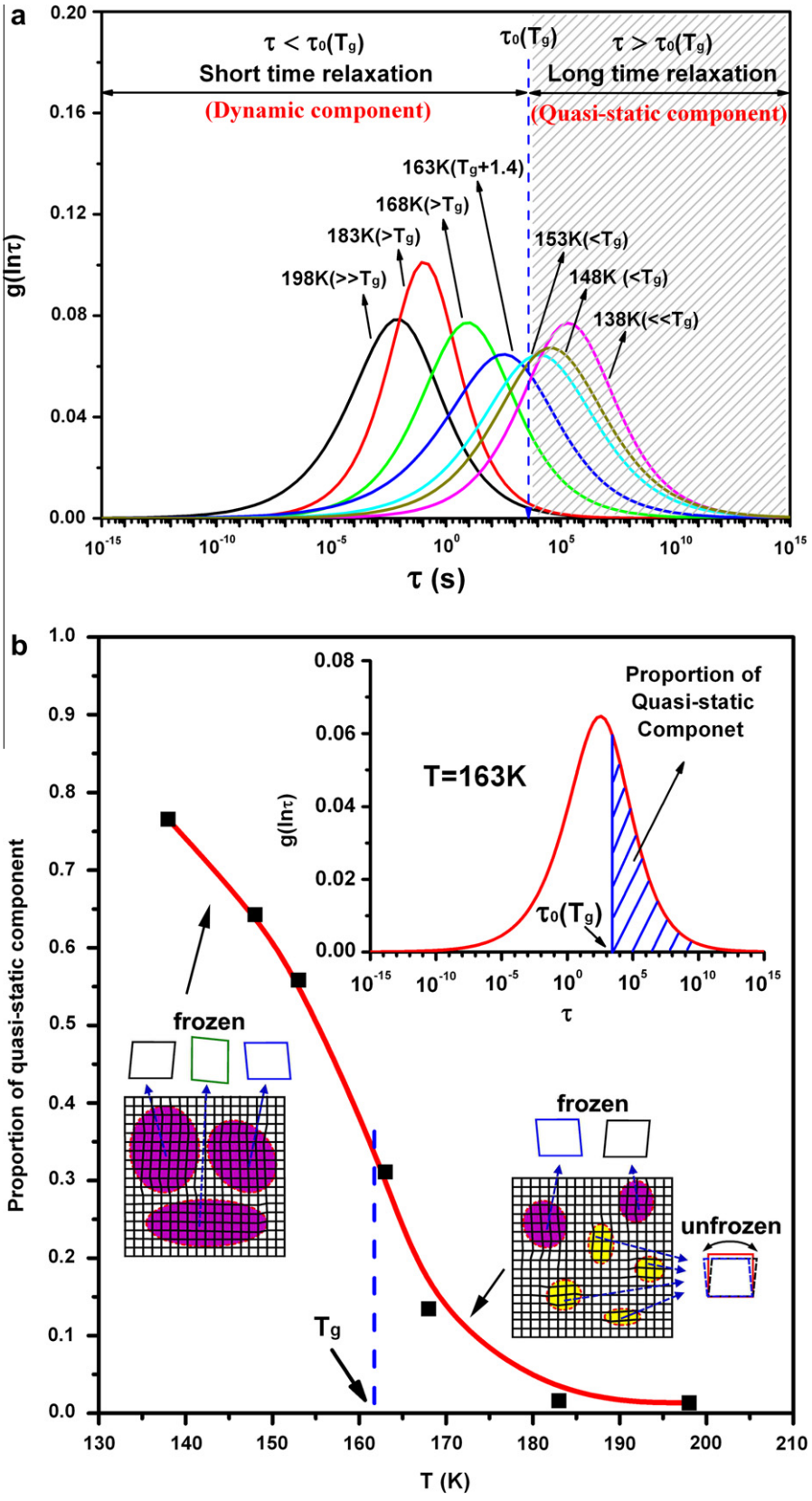

Fig. 3. (a) Evolution of the relaxation spectrum of $Ti_{48.5}Ni_{51.5}$ strain glass with temperature. (b) The quasi-static component of the relaxation spectrum of $Ti_{48.5}Ni_{51.5}$ strain glass, i.e. the proportion of the frozen martensitic nanodomains among all nanodomains. It increases continuously and shows a rapid increase around the freezing temperature T_g on cooling. The quasi-static component is obtained by calculating the "weight" of the long time relaxations ($\tau > \tau_0(T_g)$),indicated by the shaded area in the top inset. The schematic insets demonstrate that some martensitic nanodomains are frozen even above T_g and almost all the nanodomains are frozen well below T_g.

dynamic measurements demonstrated that the precursor state is essentially ergodic or dynamic [15]. The above seemingly contradictory experimental facts can be understood by considering the existence of a small portion of long lived relaxations at tens of Kelvin above M_s, which show up as the quasi-static tweed pattern (or nanodomains) while not causing a breakdown in global ergodicity in the precursor state.

The energy barrier E_a for flipping martensitic nanodomains is caused by the random local stresses generated by point defects. These random local stresses not only dictate the nanodomains of the strain glass but also hinder the rotation of each nanodomain. This results in an energy barrier E_a and, hence, in a kinetic slowing down of the evolution of the nanodomains during the strain glass transition. The origin of the temperature evolution of the relaxation spectrum for strain glasses is competition between the thermal activation energy k_BT and the energy barrier E_a for the flipping of martensitic nanodomains. At high temperatures the thermal activation energy k_BT is much larger than the energy barrier E_a, thus relaxation of the martensitic nanodomains is very fast and the corresponding relaxation spectrum is dominated by short relaxation times at these temperatures. With decreasing temperature the thermal activation energy become comparable with or even lower than the energy barrier, thus the relaxation spectrum of the strain glass shifts gradually to longer time scales on cooling.

5. Conclusion

We obtained a relaxation spectrum for a strain glass $Ti_{48.5}Ni_{51.5}$ through fitting its Cole–Cole plot of complex compliance data. Our results show that the relaxation spectrum of the strain glass evolves from a short time scale to a long time scale on cooling, resulting in the breakdown of ergodicity and dynamic frequency dispersion behavior in this system. The relaxation spectrum of the strain glass also demonstrates that the system undergoes a transition from Vogel–Fulcher kinetics to Arrhenius kinetics around the freezing temperature, which is a new glassy feature of this system. Quantitative analysis of the relaxation spectrum of the strain glass also answered two interesting questions: (i) the onset of non-ergodicty starts in the unfrozen strain glass state, and (ii) the precursory state with a quasi-static tweed pattern and nanoclusters in a martensitic system appears to be ergodic. In addition, the experimentally measured relaxation spectrum of the strain glass provides a basis for comparison with future theoretical models of this new glass phenomenon.

Acknowledgements

The present work was financially supported by a JSPS Fellowship from Japan, the National Natural Science Foundation of China (Grants Nos. 50720145101 and 50771079), the National Basic Research Program of China (Grants Nos. 2004CB619303 and 2010CB635101), the Fundamental Research Funds for Central Universities, and the NCET and 111 project of China. We thank T. Suzuki, S. Sarkar, G.L. Fan and Z. Zhang for technical support and helpful discussions.

References

[1] Mydosh JA. Spin glasses. Philadelphia (PA): Taylor & Francis; 1993.
[2] Binder K, Kob W. Glassy materials and disordered solids. London: World Scientific; 2005.
[3] Jérôme B, Commandeur J. Nature 1997;386:589.
[4] Binder K, Young AP. Rev Mod Phys 1986;58:801.
[5] Santen L, Krauth W. Nature 2000;405:550.
[6] Birge NO, Jeong YH, Nagel SR, Bhattacharya S, Susman S. Phys Rev B 1984;30:2306.
[7] Courtens E. Phys Rev Lett 1984;52:69.
[8] Pareige C, Zapolsky H, Khachaturyan AG. Phys Rev B 2007;75:054102.
[9] Su CC, Vugmeister B, Khachaturyan AG. J Appl Phys 2001;90:6345.
[10] Glazounov AE, Tagantsev AK. Appl Phys Lett 1998;73:856.
[11] Sarkar S, Ren X, Otsuka K. Phys Rev Lett 2005;95:205702.
[12] Wang Y, Ren X, Otsuka K. Phys Rev Lett 2006;97:225703.
[13] Wang Y, Ren X, Otsuka K, Saxena A. Phys Rev B 2007;76:132201.
[14] Wang Y, Ren X, Otsuka K, Saxena A. Acta Mater 2008;56:2885.
[15] Ren X et al. Philos Mag 2010;90:141.
[16] Schryvers D, Tanner L. Ultramicroscopy 1990;32:241.
[17] Murakami Y, Shindo D. Philos Mag Lett 2001;81:631.
[18] Murakami Y, Shibuya H, Shindo D. J Microscopy 2000;203:22.
[19] Alvarez F, Alegría A, Colmenero J. Phys Rev B 1991;44:7306.
[20] Hüser D, Duyneveldt AJ van, Nieuwenhuys GJ, Mydosh JA. J Phys C Solid State Phys 1986;19:3697.
[21] Daniel VV. Dielectric relaxation. London: Academic Press; 1967.
[22] Havriliak JS, Havriliak SJ. Dielectric and mechanical relaxation in materials. New York: Hanser Publishers; 1997.
[23] Ediger MD, Angell CA, Nagel SR. J Phys Chem 1996;100:13200.
[24] Semenovskaya S, Khachaturyan AG. Acta Mater 1997;45:4367.
[25] Kartha S, Castan T, Krumhansl JA, Sethna JP. Phys Rev Lett 1991;67:3630.
[26] Kartha S, Krumhansl JA, Sethna JA, Wickham LK. Phys Rev B 1995;52:803.